University of Miskolc

Faculty of Mechanical Engineering
Institute of Energy Engineering and Chemical Machinery
Department of Fluid and Heat Engineering

Vortex-induced vibrations at low Reynolds numbers

Dániel Dorogi

Booklet of the PhD Dissertation

István Sályi Doctoral School of Mechanical Engineering Sciences
Main Topic Group: Fundamental Sciences in Mechanical Engineering
Topic Group: Transport Processes and Machines

Head of Doctoral School:
Gabriella Vadászné Bognár
Doctor of Science, Full Professor

Head of Main Topic Group:
István Páczelt
Member of the Hungarian Academy of Sciences, Professor Emeritus

Head of the Topic Group:
Tibor Czibere
Member of the Hungarian Academy of Sciences, Professor Emeritus

Scientific Supervisor:
László Baranyi
Dr. habil, Full Professor

Miskolc
2020

Dániel Dorogi

Vortex-induced vibrations at low Reynolds numbers

Booklet of the PhD dissertation

Miskolc
2020

Members of the Defense Committee

Chairman
Edgár Bertóti
DSc, Full Professor, *University of Miskolc*

Member and Secretary
Betti Bolló
PhD, Associate Professor, *University of Miskolc*

Members
János Vad
DSc, Full Professor, *Budapest University of Technology and Economics*

László Kollár
PhD, Full Professor, *Eötvös Loránd University*

Károly Jármai
DSc, Full Professor, *University of Miskolc*

Reviewers
László Könözsy
PhD, Senior Lecturer, *Cranfield University*, United Kingdom

Gergely Kristóf
PhD, Associate Professor, *Budapest University of Technology and Economics*

1 Introduction

In the past few decades, due to its relevance in many engineering fields (e.g. in offshore risers, chimney stacks, and heat exchangers) several researchers investigated the fluid flow around a circular cylinder placed into a uniform stream. Periodic vortex shedding exerts a fluctuating load on the body which can induce the vibration of the cylinder. This phenomenon is referred to as *vortex-induced vibrations* (VIV) whose analyses has been the topic of many scientific papers [1–4]. Although in reality the cylinder can move both streamwise with and transverse to the free stream (i.e. in two degrees of freedom), one-degree-of-freedom motions are also commonly used to model VIV.

1.1 Transverse vortex-induced vibrations

Khalak and Williamson [2] investigated transverse-only VIV of a circular cylinder using an experimental approach. Plotting the amplitude of cylinder oscillation against reduced velocity U^*, for very low $m^*\zeta$ values they found three distinct response branches, namely the initial, the upper and the lower branches. Here m^* and ζ are the mass ratio and structural damping ratio values, respectively. Beyond a critical value of $m^*\zeta$ the upper branch disappears, only initial and lower branches remain, and this phenomenon is called two-branch response. Soti et al. [5] using laboratory measurements identified a three-branch behavior for a wide damping ratio domain; they showed the occurrence of the upper branch even at low oscillation amplitudes (down to $0.2d$, where d is the cylinder diameter).

The experimental studies are mostly carried out in the Reynolds number range of $\mathrm{Re} = O(10^3\text{–}10^4)$. However, numerical (CFD) simulations, due to the high computational time demand and the three-dimensionality of the flow [6] are usually performed in the low-Re domain [$\mathrm{Re} = O(10^2)$]. In terms of CFD simulations, to model the real-life phenomenon, the natural frequency of the cylinder is often assumed to be constant [7, 8]. This model requires a linear relationship between Re and U^*; $\mathrm{Re} = KU^*$, where K is the dimensionless natural frequency of the cylinder. However, several papers focus on the separate effects of Re and U^* [9, 10].

The results at low Reynolds numbers show that the peak oscillation amplitude is markedly lower (maximum $0.55d$, see Navrose and Mittal [10]) compared to the data in the high-Re domain (can exceed $0.8d$, see Khalak and Williamson [2]). Besides, CFD studies at low Re have not reported an upper branch even for undamped systems [9, 10]. In most of these cases, the classic 2S wake mode (two single vortices are shed from the cylinder in each motion cycle) was identified both in the initial and lower branches. Evangelinos and Karniadakis [11] reported from their two and three-dimensional computations that P+S vortex pattern (a vortex pair and a single vortex) may also be associated with the upper branch. Singh and Mittal [12] investigated two-degree-of-freedom vortex-induced vibrations and found P+S vortex structures above $\mathrm{Re} = 300$.

1.2 Streamwise vortex-induced vibrations

In the literature streamwise-only VIV received less attention, most likely because of the low amplitude of cylinder oscillation. In his review paper King [13] showed that the maximum vibration amplitude is about $0.2d$ which is very low compared to the transverse-only VIV cases. The experimental studies carried out by King [13], Aguirre [14] or Gurian et al. [15] showed that two excitation regions occur in streamwise VIV. The first branch is associated with a symmetrical shedding of vortices simultaneously from both sides of the cylinder, while in the second branch alternating vortex shedding was found.

In [13–15] measurements were carried out for Reynolds numbers above $\mathrm{Re} = 10^3$. Based on the mechanical energy transfer between the oscillating body and the surrounding fluid, Tanida et al. [16], Konstantinidis and Bouris [17], and Kim and Choi [18] concluded that vortex-induced streamwise vibrations cannot occur at low Reynolds numbers above the oscillation amplitude of $0.05d$. However, streamwise VIV of a circular cylinder at low Reynolds numbers is plausible but at lower oscillation amplitudes; below $0.05d$. The research question whether streamwise VIV is possible to occur at low Re has not yet been addressed.

1.3 Two-degree-of-freedom vortex-induced vibrations

In practice the cylinder is able to move in both streamwise and transverse directions, i.e. in two degrees of freedom. In general, the mass ratios (m_x^* and m_y^*) and the natural frequencies (f_{Nx} and f_{Ny}) are different in the two directions. Moe and Wu [19] and Sarpkaya [20] carried out experiments for $m_x^* \neq m_y^*$ in the natural frequency ratio range of $f_{Nx}/f_{Ny} = 1$–2. They found no evidence for the initial, upper and lower branches identified originally for transverse-only VIV (see Section 1.1). Jauvtis and Williamson [21] limited their measurements to the special case of $m^* = m_x^* = m_y^*$ and $f_N = f_{Nx} = f_{Ny}$. In addition to the three response branches, for $m^* < 6$ they captured the super-upper branch.

Similarly to transverse-only VIV, numerical simulations are mostly carried out at low Reynolds numbers. Although there are some studies analyzing the separate effects of Re and U^* [12], in most cases the $\mathrm{Re} = KU^*$ model is employed [22, 23]. It can be seen in the literature that the investigations are limited to low dimensionless natural frequency values ($K < 16.6$ for two-degree-of-freedom VIV). To the best knowledge of the author, the research question regarding the effect of K on the cylinder response has not yet been addressed.

For two-degree-of-freedom VIV the path of the cylinder is another area of interest. Based on the relevant literature, figure-eight motion is the most common path for a freely vibrating cylinder placed into a uniform stream [12, 22]. In addition, there are some cases where the cylinder follows an orbital trajectory. These include but are not limited to the cases when the natural frequencies of the cylinder in the two directions are different [24], when the cylinder is pivoted [25], or when the body is placed into a shear flow [26]. To the best knowledge of the author, the occurrence of an orbital motion has not

yet been specified for a single isolated cylinder placed into a uniform stream considering low Reynolds numbers.

2 Objectives of the research

Based on the review of the relevant literature, different research questions are addressed which determine the objectives of this dissertation. The research questions and the objectives are detailed in the following points.

Objective 1

In the first part of the dissertation two-degree-of-freedom vortex-induced vibrations of a circular cylinder are investigated. For this analysis a cylinder elastically supported in both streamwise and transverse directions is used which layout is shown in Fig. 1a. This is described in Sections 1.1 and 1.3 that the natural frequency of the cylinder is often assumed to be constant. For these cases the Reynolds number is varied linearly with the reduced velocity. As was pointed out earlier, this type of computation is limited to low dimensionless natural frequency values, i.e. to $K < 16.6$ for two-degree-of-freedom VIV. The first research question addressed in this dissertation is as follows:

What are the effects of the dimensionless natural frequency K on the cylinder response and aerodynamic force coefficients?

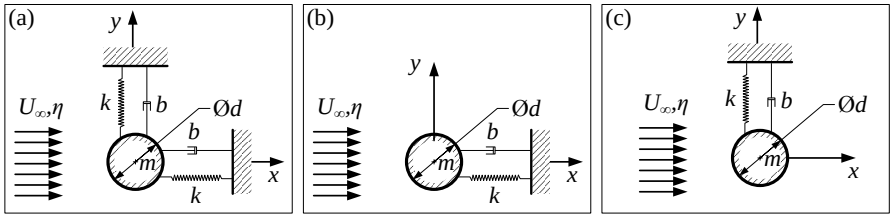

Figure 1. Circular cylinder elastically supported in both streamwise and transverse directions (a), only in streamwise direction (b), and only in transverse direction (c)

Objective 2

Singh and Mittal [12] carried out computations at the fixed reduced velocity of $U^* = 4.92$ in the Reynolds number range $50 \leq \mathrm{Re} \leq 500$ considering two-degree-of-freedom VIV of a circular cylinder. They showed that varying the Reynolds number over $\mathrm{Re} = 300$, the asymmetrical P+S wake mode occurs, which is rarely identified in vortex-induced vibration cases. Thus, the following research questions are addressed:

Does P+S wake mode occur at high dimensionless natural frequency values? What is the effect of this asymmetrical mode on the cylinder path?

Objective 3

In the next part of the dissertation streamwise-only VIV is analyzed (see the layout in Fig. 1b). The forced vibration studies revealed that vortex-induced streamwise vibration of a circular cylinder is not feasible at low Reynolds numbers above the oscillation amplitude value of $0.05d$ [16–18] (see relevant discussion in Section 1.2). However, there are no data available in the literature whether streamwise VIV occurs at low Re but at lower amplitudes of cylinder vibration; i.e. below $0.05d$. Hence, in this part of the research project the following questions are addressed:

Is it possible for streamwise-only VIV to occur in the low-Re domain? What are the effects of m^* and Re on the cylinder response?

Objective 4

In the closing part of the PhD dissertation transverse-only free vibrations of a circular cylinder are analyzed (see the layout in Fig. 1c). It was pointed out in Section 1.1 that an upper branch has not yet been observed in the low-Reynolds number domain. However, there are some results available in the literature which suggest that the upper branch can occur at low Reynolds numbers (see Section 1.1 and the dissertation for further details). For this reason the following research questions are addressed:

Does the upper branch (i.e. the three-branch cylinder response) occur at the Reynolds number of 300? What is the effect of structural damping on the cylinder response?

3 Methodology

In this dissertation systematic two-dimensional CFD computations are performed to answer the research questions addressed in Section 2. The governing equations of the incompressible constant-property Newtonian fluid flow are the two components of the Navier-Stokes equations written in a non-inertial frame of reference attached to the oscillating cylinder, the continuity equation, and the pressure Poisson equation. Solving for the instantaneous cylinder displacements, and velocity and acceleration components, the two structural equations are used (see Singh and Mittal [12]). In order to avoid numerical inaccuracies, the governing equations and the boundary conditions are transformed into the computational domain where the equations are solved using the finite difference method. For further details of the CFD approach the reader is referred to Baranyi [27] and the dissertation.

The first step of the research was to carry out independence studies in order to determine the optimal combination of the computational parameters which is the best compromise between accuracy and computational time. Using these parameters, step-by-step validation is carried out. The comparison of the results obtained in this dissertation showed very good agreement against the data presented in Bourguet and Lo Jacono [28] and Navrose and Mittal

[10] for transverse-only vortex-induced vibrations, in Bourguet and Lo Jacono [29] for self-excited streamwise vibrations, and in Prasanth and Mittal [22], He and Zhang [30], and Bao et al. [31] for two-degree-of-freedom VIV cases.

4 Analyses performed

After verification and validation of the numerical approach, systematic computations are carried out to accomplish the objectives shown in Section 2.

4.1 Two-degree-of-freedom vortex-induced vibrations

I started my PhD research with the analyses of two-degree-of-freedom vortex-induced vibrations. In order to answer the research questions addressed in **Objectives 1** and **2**, systematic computations are performed at different constant dimensionless natural frequency values between $K \cong 12$ and 44. The Reynolds number is varied in the range of $60 \leq \mathrm{Re} \leq 250$ (corresponding to the variation of K), while the mass ratio and the structural damping ratio are fixed at $m^* = 10$ and $\zeta = 0\%$, respectively. The new scientific results regarding these computations are summarized in **Contributions 1** and **2**.

4.2 Streamwise-only vortex-induced vibrations

The research questions addressed in **Objective 3** is related to the analysis of streamwise-only VIV. In order to answer these questions, two sets of computations are carried out. First, simulations are performed at the mass ratio values $m^* = 2, 5, 10$, and 20, while keeping the Reynolds number constant at $\mathrm{Re} = 180$. A model based on harmonic assumptions is used to explain the phenomenon observed in the numerical results. Second, computations are carried out at different Reynolds numbers ($\mathrm{Re} = 100, 180$, and 250), while keeping the mass ratio constant at $m^* = 10$. In both sets of computations the reduced velocity is varied between $U^* = 1.5$ and 3.5, while the structural damping ratio is fixed at zero. The novel results from these CFD simulations are included in **Contributions 3** and **4**.

4.3 Transverse-only vortex-induced vibrations

Finally, to answer the research questions addressed in **Objective 4**, computations are performed for transverse-only free vibrations of a circular cylinder. The CFD simulations are carried out at the Reynolds number and mass ratio values of $\mathrm{Re} = 300$ and $m^* = 10$, respectively. Damping ratio between $\zeta = 0\%$ and 5% is considered, that is, the combined mass-damping parameter is chosen to be in the range of $m^*\zeta = 0$ and 0.5. The reduced velocity is varied from $U^* = 2.5$ to 7.5. Similarly to the self-excited streamwise vibration analyses, the harmonic oscillator model is used to explain the phenomena observed in the numerical data. **Contributions 5** and **6** include the new scientific results obtained from these sets of simulations.

5 New scientific results

Contribution 1

The CFD simulations for two-degree-of-freedom vortex-induced vibrations of a circular cylinder at constant dimensionless natural frequency values K are limited to the range of $K < 16.6$. By performing computations at different K values between $K \cong 12$ and 35 ($m^* = 10$, $\zeta = 0\%$, and $\mathrm{Re} = 60$–250) it was found that

(a) Plotting the data sets belonging to different K values against $U^*\mathrm{St}$ makes the comparison easier than using Re as an independent parameter.

(b) Local peak values are found in the rms of streamwise cylinder displacement $x_{0'}$ and streamwise fluid force coefficient $C_{x'}$ at around $U^*\mathrm{St} = 0.47$ for $K \cong 16.6$–34.7. The local maximum values in $x_{0'}$ and $C_{x'}$ are found to increase with K.

(c) For K values between $K \cong 16.6$ and 34.7 $C_{x'}$ approaches zero in the vicinity of $U^*\mathrm{St} = 0.5$, in the same location where the phase difference of C_x relative to x_0 changes abruptly from 0° to 180°.

(d) The pressure streamwise fluid force coefficient C_{xp} is responsible for the abrupt phase change between C_x and x_0 identified for values in $K \cong 16.6$–34.7, because the phase angle between C_{xp} and x_0 suddenly shifts from 0° to 180° at $U^*\mathrm{St} \cong 0.5$, and the phase difference of the viscous streamwise fluid force coefficient C_{xv} relative to x_0 slowly increases; in the vicinity of $U^*\mathrm{St} = 0.5$ its value is about 54°. For the dimensionless natural frequency values in $K \cong 16.6$–34.7 the limit cycle curve (C_{xv}, C_{xp}) switches from clockwise to counterclockwise orientation at $U^*\mathrm{St} \cong 0.5$, due to the sudden change in the phase angle between C_{xp} and x_0.

(e) For K values in $K \cong 16.6$–34.7 the orientation of the cylinder path switches also from clockwise to counterclockwise orbit (in the upper loop of the figure-eight path) at around $U^*\mathrm{St} = 0.5$.

Related publication: Dorogi and Baranyi [J1]

Contribution 2

The P+S asymmetrical vortex structures are rarely identified for vortex-induced vibrations of a circular cylinder. This wake mode is expected to occur at high dimensionless natural frequency values. Using CFD computations for two-degree-of-freedom VIV at different K values between $K \cong 35$ and 44 ($m^* = 10$, $\zeta = 0\%$, and $\mathrm{Re} = 60$–250) it was found that

(a) The dimensionless natural frequency strongly influences the path of the cylinder. While below $K \cong 36.6$ only distorted figure-eight motions are observed, between $K \cong 36.6$ and 43.7 in a thin $U^*\mathrm{St}$ domain orbital

trajectories (i.e. raindrop-shaped orbits) are identified whose U^*St range widens with K.

(b) The raindrop-shaped paths are asymmetrical orbits, because the frequency spectra of the streamwise vibration component contain two high-intensity peaks corresponding to f_y^* and $2f_y^*$. Here f_y^* is the dimensionless transverse oscillation frequency of the cylinder.

(c) P+S asymmetrical vortex structures are found in the wake of the cylinder for orbital paths, while 2S or C(2S) modes are identified for distorted figure-eight motion cases. Here P and S refer to vortex pair and single vortex shed form the body, respectively, and C refers to the coalescence of the positive and negative vortices.

(d) A hysteresis loop is identified close to the boundary, where the vortex structure switches from P+S to 2S mode, as well as the cylinder orbit changes between raindrop-shaped and distorted figure-eight paths. It was shown that increasing U^* together with Re in the range of $0.97 < U^* \leq 1.01$, orbital trajectories and P+S modes are formed, while decreasing U^* and Re in the same domain, distorted figure-eight paths and 2S modes occur.

(e) For raindrop-shaped orbits the time-mean values of the transverse fluid force coefficient is $\left|\overline{C}_y\right| > 0$, because the P+S wake mode means an asymmetrical load on the cylinder surface. For these cases $\overline{C}_y$ jumps abruptly between two solutions, which are symmetrical, because the (C_x, C_y) and (x_0, y_0) limit cycles in the pre- and post-jump cases are mirror images of each other.

Related publications: Dorogi and Baranyi [J2], Dorogi and Baranyi [C5], and Dorogi and Baranyi [C6]

Contribution 3

In the literature streamwise-only vortex-induced vibrations of a circular cylinder have been found only for Reynolds number values above $\mathrm{Re} = 10^3$.

(a) Using two-dimensional CFD computations I showed that streamwise-only vortex-induced vibrations of a circular cylinder are possible to occur also at low Reynolds numbers. A single excitation region is observed for all Reynolds number and mass ratio combinations investigated ($m^* = 2, 5, 10$, and 20 at $\mathrm{Re} = 180$, and $\mathrm{Re} = 100, 180$, and 250 at $m^* = 10$). The dimensionless oscillation amplitude $\hat{x}_0$ plotted against the reduced velocity U^* increases up to a peak value, beyond which it gradually decreases. The nondimensional frequency of cylinder vibration f_x^* behaves oppositely: it decreases to its minimum value, then it monotonically increases. It was shown that the dimensionless vibration frequency is always lower than the double of the Strouhal number for a

stationary cylinder. This finding is consistent with the forced vibration results available in the literature.

(b) For a given (Re, m^*) combination the peak value in $\hat{x}_0$ and the minimum in f_x^* are identified approximately at the same U^* value. Varying the mass ratio from $m^* = 2$ to 20, although the location of the peak response shifts to higher reduced velocity values (from $U^* = 2.17$ to 2.61), the maximum $\hat{x}_0$ and the minimum f_x^* stay approximately constant. However, when Re is increased between 100 and 250 the U^* value where the peak response is identified decreases from $U^* = 2.9$ to 2.47. In contrast to the different m^* cases, the peak $\hat{x}_0$ value increases intensively with Re; for the Reynolds number values of $\mathrm{Re} = 100, 180$, and 250 the peak vibration amplitudes are approximately 0.22%, 1.1%, and 2.3% of the cylinder diameter, respectively.

(c) I showed also that the single excitation region identified in this dissertation corresponds to the second response branch found in the high-Re experiments, because alternating modes of vortex shedding are observed in all investigated cases.

Related publications: Dorogi et al. [C9], Dorogi et al. [C10], and Konstantinidis et al. [C12]

Contribution 4

Assuming that the streamwise cylinder displacement x_0 and the streamwise fluid force coefficient C_x are sinusoidal functions of time, the following formula is obtained for the amplitude of C_x:

$$\hat{C}_x = \frac{2\pi^3 m^* \hat{x}_0}{U^{*2}} \sqrt{(1 - f_x^{*2} U^{*2})^2 + 4\zeta^2 f_x^{*2} U^{*2}},$$

where m^* and ζ are the mass ratio and damping ratio values, respectively, $\hat{x}_0$ and f_x^* are the dimensionless oscillation amplitude and frequency values, and U^* is the reduced velocity. This expression shows that for $\zeta = 0\%$, $\hat{C}_x$ becomes zero at the point where the vibration frequency coincides with the natural frequency of the cylinder, i.e. at $f_x^* U^* = 1$. This finding was confirmed using CFD simulations where the cylinder was restricted to move only streamwise with the uniform stream. The computations at $\mathrm{Re} = 180$ and $m^* = 2, 5, 10$, and 20 revealed that $\hat{C}_x \to 0$ at $U^* \cong 2.625$. The streamwise fluid force coefficient has strongly non-harmonic nature in the vicinity of $U^* = 2.625$, because $\hat{x}_0$ is non-zero at this point. A frequency component double the frequency of cylinder vibration (i.e. the second harmonic component) occurs just before the point of $\hat{C}_x \to 0$. At the reduced velocity value, where the vibration frequency is identical to the natural frequency of the cylinder, the intensity of the second harmonic component is the highest.

For undamped vibration cases the phase difference of C_x relative to x_0 switches suddenly between 0° and 180° at $\hat{C}_x \to 0$. Besides, the phase lag

of the transverse fluid force with respect to the cylinder displacement displays a gradual increase (instead of abrupt jump) from approximately 20° to 110°. This gradual increase can be attributed to shift in the timing of vortex shedding, which was confirmed using the instantaneous vorticity contours.

Related publications: Dorogi et al. [C9], Dorogi et al. [C10], and Konstantinidis et al. [C12]

Contribution 5

Up till now an upper branch (i.e. a three-branch cylinder response) has been reported only for high-Reynolds number flows ($\mathrm{Re} = 10^3$–10^4). Using two-dimensional CFD simulations for transverse-only VIV of a circular cylinder, a three-branch cylinder response is observed at the Reynolds number, mass ratio and structural damping ratio values of $\mathrm{Re} = 300$, $m^* = 10$, and $\zeta = 0\%$, respectively. The initial branch takes place in the range of $3.45 < U^* \leq 4$, the upper branch is observed between $U^* = 4$ and 4.89, and the lower branch occurs in the domain of $4.89 < U^* \leq 5.9$. The time-averaged phase differences of the vortex force and the transverse fluid force relative to the cylinder displacement show gradual variations between approximately 0° and 180° at the upper and lower boundaries of the upper branch, respectively. Irregular changes (phase slips and unbounded increase/decrease) are observed in the time-dependent phase angle values which explain the gradual and not abrupt variations in the time-mean values.

Increasing the structural damping ratio leads to the transition from three-branch to two-branch response. This finding is comparable to the experimental results (available in the literature) at high Reynolds numbers. In the domain of $\zeta \leq 1\%$ the upper branch is found to occur whose reduced velocity range ΔU^*_{UB} decreases with the damping ratio (e.g. $\Delta U^*_{UB} = 0.88$ for $\zeta = 0\%$, while $\Delta U^*_{UB} = 0.31$ for $\zeta = 1\%$). For $\zeta = 3\%$ and 5%, the upper branch completely disappears from the response, only the initial and lower branches remain.

Related publications: Dorogi and Baranyi [J4], Dorogi and Baranyi [C7], Dorogi and Baranyi [C8] és Dorogi et al. [C11]

Contribution 6

At $(\mathrm{Re}, m^*, \zeta) = (300, 10, 0\%)$ an upper branch has been identified for transverse-only VIV of a circular cylinder.

(a) At the higher boundary of the upper branch (from $U^* = 4.7$ to 4.89) the time-dependent phase difference of the transverse fluid force coefficient C_y relative to the cylinder displacement y_0 (i.e. the transverse phase) increases roughly uniformly with time. This effect is closely related to the large detuning value between the frequencies of cylinder vibration f^*_y and transverse fluid force coefficient $f^*_{C_y}$. In the domain of $U^* = 4.7$–4.89, $f^*_y - f^*_{C_y} \cong -0.2$, which in absolute value is close to the Strouhal number

St for a stationary cylinder at $\mathrm{Re} = 300$. Since $f_y^* \cong \mathrm{St}$ between $U^* = 4.7$ and 4.89, the detuning value $f_y^* - f_{C_y}^* \cong -\mathrm{St}$ can only be achieved when $f_{C_y}^* = 2f_y^* \cong 2\mathrm{St}$. This finding was shown explicitly using FFT analysis; the second harmonic frequency component is the most intensive peak in the spectra of C_y between $U^* = 4.7$ and 4.89 for $\zeta = 0\%$.

(b) Increasing the structural damping ratio value up to $\zeta = 0.5\%$, $f_y^* - f_{C_y}^* = 0$ in the entire reduced velocity domain, hence the time-dependent transverse phase no longer shows an unbounded increase at the higher end of the upper branch. This effect implies that the role of the second harmonic frequency component in the spectra of C_y decreases with the structural damping ratio. The spectral analyses of C_y showed that the intensity of the second harmonic component was negligible just before the jump to the lower branch.

(c) The currently obtained CFD data belonging to the various structural damping ratio values (between $\zeta = 0\%$ and 5%) were compared to the results from the harmonic oscillator model. It was shown that the computational data and the harmonic model results compare very well at the beginning of the upper branch and in the lower branch. However, at the end of the upper branch the CFD data and the harmonic model results are far from each other. This finding confirms my previous statement concerning the non-harmonic nature of the transverse fluid force at the end of the upper branch.

Related publications: Dorogi and Baranyi [J4], Dorogi and Baranyi [C7], Dorogi and Baranyi [C8] és Dorogi et al. [C11]

6 Possible applications of the results

Nowadays civil engineers take the effect of vortex shedding into account during the designing processes of tall slender buildings, towers, silos, bridges or offshore structures. Besides, flow around bluff bodies play important role in heat exchangers, transmission lines, risers or masts. One can argue that in these applications Reynolds number can exceed several thousand which is much higher than the cases investigated in this dissertation ($\mathrm{Re} \leq 300$). However, it has been shown in the literature that the effect of Re on the flow field is not so strong; simulations at low Reynolds numbers can predict the phenomenon at high Re quite well.

I believe that the results presented in this dissertation are useful in an academic point of view. The analyses of single-degree-of-freedom VIV showed that self-excited streawise motion and the occurrence of an upper branch for transverse-only free vibrations are possible at low Reynolds numbers which has not yet been presented in the literature. Additional analyses of the results can provide further insight into the source of vortex-induced vibrations.

At present I am thinking about setting up a new course material about fluid-structure interaction in which the current results or investigation methods can also be included.

7 Future plans

Although in this dissertation several analyses are carried out for one- and two-degree-of-freedom vortex-induced vibrations at low Reynolds numbers, there are still a lot of unanswered questions for further investigation. The topics related directly to my research are summarized in the following points:

- **Contributions 1** and **2** show new scientific results for two-degree-of-freedom VIV when the natural frequencies of the cylinder in streamwise and transverse directions f_{Nx} and f_{Ny} are identical. The question arises what the effect of the natural frequency ratio FR $= f_{Nx}/f_{Ny}$ is on the cylinder response. Preliminary results are available in this topic in Dorogi and Baranyi [J3], indicating that FR highly influences the cylinder path, but additional computations are required.

- **Contributions 3** and **4** show that a single excitation region occurs for streamwise-only vortex-induced vibrations in the low-Reynolds number domain. However, at moderately high Re two response branches have been identified. In order to investigate how the response switches between one-branch and two-branch responses, three-dimensional computations are needed.

- It was shown in **Contributions 5** and **6** that a separate upper branch occurs at the Reynolds number of 300. However, at lower Re (e.g. at Re $= 100$) two response branches (i.e. the initial and lower branches) have been reported in the literature. I aim to perform CFD computations at different Reynolds numbers ranging between Re $= 50$ and 300 to find the critical Reynolds number value Re_c, above which three-branch response occurs, but at $\mathrm{Re} < \mathrm{Re}_c$ only the initial and lower branches can be identified.

During the literature review I realized that vortex-induced vibrations of a circular cylinder placed into an oscillatory flow received little attention. However, it appears in many engineering fields, for example wave motions are commonly modeled with oscillatory flows. To my best knowledge, very few papers examine this problem numerically. For this reason, systematic CFD computations are planned in this field in the near future.

The author's publications in the topic of the dissertation

Journal papers

[J1] Dorogi, D. and Baranyi, L., 2018. Numerical simulation of a freely vibrating circular cylinder with different natural frequencies. *Ocean Engineering* **158**, 196–207. DOI: 10.1016/j.oceaneng.2018.03.079.

[J2] Dorogi, D. and Baranyi, L., 2019. Occurrence of orbital cylinder motion for flow around freely vibrating circular cylinder in uniform stream. *Journal of Fluids and Structures* **87**, 228–246. DOI: 10.1016/j.jfluidstructs.2019.03.004.

[J3] Dorogi, D. and Baranyi, L., 2019. Sajátfrekvencia-hányados hatása a szabadrezgést végző körhenger körüli folyadékáramlásra (Effects of natural frequency ratio on fluid flow around a freely vibrating circular cylinder). *Jelenkori Társadalmi és Gazdasági Folyamatok* **14**(1), 19–27.

[J4] Dorogi, D. and Baranyi, L., Identification of upper branch for vortex-induced vibration of a circular cylinder at Re=300. *Submitted to Journal of Fluids and Structures.*

[J5] Konstantinidis, E., Dorogi, D., and Baranyi, L., Resonance in vortex-induced in-line vibration at low Reynolds numbers. *Submitted to Journal of Fluid Mechanics.*

Conference Papers

[C1] Dorogi, D. and Baranyi, L., 2016. Effect of gradual amplitude increase on flow around a cylinder oscillated in line. In: *Proceedings of the* 4^{th} *International Scientific Conference on Advances in Mechanical Engineering (ISCAME 2016).* Debrecen, Hungary, pp. 151–156.

[C2] Dorogi, D. and Baranyi, L., 2017. Elastically supported cylinder in two-degree-of-freedom motion: a numerical study. In: *Proceedings of the MultiScience – XXXI. microCAD International Multidisciplinary Scientific Conference (microCAD).* Miskolc, Hungary, pp. 93–100.

[C3] Dorogi, D. and Baranyi, L., 2017. Numerical simulation of flow and heat transfer for a cylinder in free vibration. In: *Proceedings of the MultiScience – XXXI. microCAD International Multidisciplinary Scientific Conference (microCAD).* Miskolc, Hungary, pp. 101–108.

[C4] Dorogi, D. and Baranyi, L., 2018. Effect of streamwise and transverse damping on flow around an elastically supported cylinder. In: *Proceedings of the Conference on Modelling Fluid Flow (CMFF'18).* Budapest, Paper number: 21, pp. 1–8.

[C5] Dorogi, D. and Baranyi, L., 2018. Natural frequency effect on the path of an elastically supported circular cylinder. In: *Proceedings of the Conference on Modelling Fluid Flow (CMFF'18).* Budapest, Paper number: 89, pp. 1–8.

[C6] Dorogi, D. and Baranyi, L., 2018. Numerical investigation of the path of a freely vibrating circular cylinder at high reduced frequency value. In: *Proceedings of the* 7^{th} *Conference on Bluff Body Wakes and Vortex-Induced Vibrations (BBVIV7).* Carry-le-Rouet, France, pp. 121–124.

[C7] Dorogi, D. and Baranyi, L., 2019. Investigation of the branching behavior of a freely vibrating circular cylinder at low Reynolds numbers. In: *Proceedings of the* 4^{th} *International Conference on Multi-scale Computational Methods for Solids and Fluids (ECCOMAS MSF 2019).* Sarajevo, Bosnia-Herzegovina, pp. 108–111.

[C8] Dorogi, D. and Baranyi, L., 2019. Szabadrezgést végző körhenger körüli áramlás numerikus vizsgálata: a csillapítási tényező hatása (Damping effects for a freely vibrating cylinder in transverse direction: a CFD study). In: *Proceedings of the* 27^{th} *International Conference on Mechanical Engineering (OGÉT2019).* Oradea, Romania, pp. 99–102.

[C9] Dorogi, D., Baranyi, L., and Konstantinidis, E., 2019. Effect of mass ratio on in-line vortex induced vibrations at a low Reynolds number. In: *Proceedings of the Flow-Structure Sound Interactions and Control (FSSIC2019).* Chania, Crete Island, Greece, Paper number: 90, pp. 1–5.

[C10] Dorogi, D., Konstantinidis, E., and Baranyi, L., 2019. Numerical investigation of streamwise vortex-induced vibration at low Reynolds numbers: mass ratio effects. In: *Proceedings of the* 4^{th} *International Conference on Multi-scale Computational Methods for Solids and Fluids (ECCOMAS MSF 2019).* Sarajevo, Bosnia-Herzegovina, pp. 112–115.

[C11] Dorogi, D., Baranyi, L., and Konstantinidis, E., Effect of damping ratio on the existence of upper branch in vortex induced vibrations at low Reynolds number. In: *Accepted for publication in the Proceedings of the* 12^{th} *International Conference on Flow-Induced Vibration.* Paris-Saclay.

[C12] Konstantinidis, E., Dorogi, D., and Baranyi, L., Aspects of vortex-induced in-line vibration at low Reynolds numbers. In: *Accepted for publication in the Proceedings of the* 12^{th} *International Conference on Flow-Induced Vibration.* Paris-Saclay.

References

[1] Bearman, P., 1984. Vortex shedding from oscillating bluff bodies. *Annual Review of Fluid Mechanics* **16**, 195–222. DOI: 10.1146/annurev.fl.16.010184.001211.

[2] Khalak, A. and Williamson, C., 1999. Motions, forces and mode transitions in vortex-induced vibrations at low mass-damping. *Journal of Fluids and Structures* **13**(7-8), 813–851. DOI: 10.1006/jfls.1999.0236.

[3] Sarpkaya, T., 2004. A critical review of the intrinsic nature of the vortex-induced vibrations. *Journal of Fluids and Structures* **19**(4), 389–447. DOI: 10.1016/j.jfluidstructs.2004.02.005.

[4] Williamson, C. and Govardhan, R., 2004. Vortex-induced vibration. *Annual Review of Fluid Mechanics* **36**, 413–455. DOI: 10.1146/annurev.fluid.36.050802.122128.

[5] Soti, A., Zhao, J., Thompson, M., Sheridan, J., and Bhardwaj, R., 2018. Damping effects on vortex-induced vibration of a circular cylinder and implications for power extraction. *Journal of Fluids and Structures* **81**, 289–308. DOI: 10.1016/j.jfluidstructs.2018.04.013.

[6] Barkley, D. and Henderson, R., 1996. Three dimensional Floquet stability analysis of the wake of a circular cylinder. *Journal of Fluid Mechanics* **322**, 215–241. DOI: 10.1017/S0022112096002777.

[7] Willden, R. and Graham, J., 2006. Three distinct response regimes for transverse vortex-induced vibrations of circular cylinders at low Reynolds numbers. *Journal of Fluids and Structures* **22**(6-7), 885–895. DOI: 10.1016/j.jfluidstructs.2006.04.005.

[8] Bahmani, M. and Akbari, H., 2010. Effects of mass and damping ratios on VIV of a circular cylinder. *Ocean Engineering* **37**, 511–519. DOI: 10.1016/j.oceaneng.2010.01.004.

[9] Leontini, J., Thompson, M., and Hourigan, K., 2006. The beginning of branching behavior of vortex-induced vibration during two-dimensional flow. *Journal of Fluids and Structures* **22**(6-7), 857–864. DOI: 10.1016/j.jfluidstructs.2006.04.003.

[10] Navrose and Mittal, S., 2017. A new regime of multiple states in free vibration of a cylinder at low Re. *Journal of Fluids and Structures* **68**, 310–321. DOI: 10.1016/j.jfluidstructs.2016.11.003.

[11] Evangelinos, C. and Karniadakis, G. E., 1999. Dynamics and flow structures in the turbulent wake of rigid and flexible cylinders subject to vortex-induced vibrations. *Journal of Fluid Mechanics* **400**, 91–124. DOI: 10.1017/S0022112099006606.

[12] Singh, S. and Mittal, S., 2005. Vortex-induced oscillations at low Reynolds numbers: hysteresis and vortex-shedding modes. *Journal of Fluids and Structures* **20**(8), 1085–1104. DOI: 10.1016/j.jfluidstructs.2005.05.011.

[13] King, R., 1977. A review of vortex shedding research and its application. *Ocean Engineering* **4**(3), 141–171. DOI: https://doi.org/10.1016/0029-8018(77)90002-6.

[14] Aguirre, J. Flow-induced in-line vibrations of a circular cylinder. PhD dissertation. Imperial College of Science and Technology, 1977.

[15] Gurian, T., Currier, T., and Modarres-Sadeghi, Y., 2019. Flow force measurements and the wake transition in purely inline vortex-induced vibration of a circular cylinder. *Physical Review Fluids* **4**(3), 034701 (17 pages). DOI: 10.1103/PhysRevFluids.4.034701.

[16] Tanida, Y., Okajima, A., and Watanabe, Y., 1973. Stability of a circular cylinder oscillating in uniform flow or in a wake. *Journal of Fluid Mechanics* **61**(4), 769–784. DOI: 10.1017/S0022112073000935.

[17] Konstantinidis, E. and Bouris, D., 2017. Drag and inertia coefficients for a circular cylinder in steady plus low-amplitude oscillatory flows. *Applied Ocean Research* **65**, 219–228. DOI: 10.1016/j.apor.2017.04.010.

[18] Kim, K.-H. and Choi, J.-I., 2019. Lock-in regions of laminar flows over a streamwise oscillating circular cylinder. *Journal of Fluid Mechanics* **858**, 315–351. DOI: 10.1017/jfm.2018.787.

[19] Moe, G. and Wu, Z.-J., 1990. The lift force on a cylinder vibrating in a current. *Journal of Offshore Mechanics and Arctic Engineering* **112**(4), 297–303. DOI: 10.1115/1.2919870.

[20] Sarpkaya, T., 1995. Hydrodynamic damping, flow-induced oscillations, and biharmonic response. *Journal of Offshore Mechanics and Arctic Engineering* **117**(4), 232–238. DOI: 10.1115/1.2827228.

[21] Jauvtis, N. and Williamson, C. H. K., 2004. The effect of two degrees of freedom on vortex-induced vibration at low mass and damping. *Journal of Fluid Mechanics* **509**, 23–62. DOI: 10.1017/S0022112004008778.

[22] Prasanth, T. and Mittal, S., 2008. Vortex-induced vibrations of a circular cylinder at low Reynolds numbers. *Journal of Fluid Mechanics* **594**, 463–491. DOI: 10.1017/S0022112007009202.

[23] Mittal, S. and Singh, S., 2005. Vortex-induced vibrations at subcritical Re. *Journal of Fluid Mechanics* **534**, 185–194. DOI: 10.1017/S0022112005004635.

[24] Kang, S., 2006. Uniform-shear flow over a circular cylinder at low Reynolds numbers. *Journal of Fluids and Structures* **22**, 541–555. DOI: 10.1016/j.jfluidstructs.2006.02.003.

[25] Kheirkhah, S., Yarusevych, S., and Narasimhan, S., 2012. Orbiting response in vortex-induced vibrations of a two-degree-of-freedom pivoted circular cylinder. *Journal of Fluids and Structures* **28**, 343–358. DOI: 10.1016/j.jfluidstructs.2011.08.014.

[26] Gsell, S., Bourguet, R., and Braza, M., 2017. Vortex-induced vibrations of a cylinder in planar shear flow. *Journal of Fluid Mechanics* **825**, 353–384. DOI: 10.1017/jfm.2017.386.

[27] Baranyi, L., 2008. Numerical simulation of flow around an orbiting cylinder at different ellipticity values. *Journal of Fluids and Structures* **24**(6), 883–906. DOI: 10.1016/j.jfluidstructs.2007.12.006.

[28] Bourguet, R. and Lo Jacono, D., 2014. Flow-induced vibrations of a rotating cylinder. *Journal of Fluid Mechanics* **740**, 342–380. DOI: 10.1017/jfm.2013.665.

[29] Bourguet, R. and Lo Jacono, D., 2015. In-line fow-induced vibrations of a rotating cylinder. *Journal of Fluid Mechanics* **781**, 127–165. DOI: 10.1017/jfm.2015.477.

[30] He, T. and Zhang, K., 2017. An overview of the combined interface boundary condition method for fluid-structure interaction. *Archives of Computational Methods in Engineering* **24**(4), 891–934. DOI: 10.1007/s11831-016-9193-0.

[31] Bao, Y., Huang, C., Zhou, D., Tu, J., and Han, Z., 2012. Two-degree-of-freedom flow-induced vibrations on isolated and tandem cylinders with varying natural frequency ratios. *Journal of Fluids and Structures* **35**, 50–75. DOI: 10.1016/j.jfluidstructs.2012.08.002.